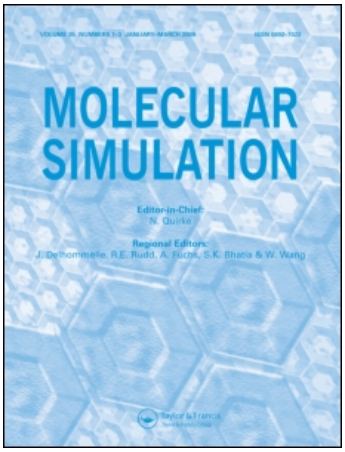

Molecular Simulation
Publication details, including instructions for authors and subscription information:
http://www.informaworld.com/smpp/title~content=t713644482

A continuum-atomistic method for incorporating Joule heating into classical molecular dynamics simulations

Clifford W. Padgett[a]; Donald W. Brenner[a]
[a] Department of Materials Science and Engineering, North Carolina State University, Raleigh, NC, USA

To cite this Article Padgett, Clifford W. and Brenner, Donald W.(2005) 'A continuum-atomistic method for incorporating Joule heating into classical molecular dynamics simulations', Molecular Simulation, 31: 11, 749 — 757
To link to this Article: DOI: 10.1080/08927020500262614
URL: http://dx.doi.org/10.1080/08927020500262614

Molecular Simulation, Vol. 31, No. 11, 15 September 2005, 749–757

Taylor & Francis
Taylor & Francis Group

A continuum-atomistic method for incorporating Joule heating into classical molecular dynamics simulations

CLIFFORD W. PADGETT* and DONALD W. BRENNER

Department of Materials Science and Engineering, North Carolina State University, Raleigh, NC 27695-7907, USA

(Received June 2005; in final form July 2005)

A hybrid atomistic-continuum method is presented for incorporating Joule heating into large-scale molecular dynamics (MD) simulations. When coupled to a continuum thermostat, the method allows resistive heating and heat transport in metals to be modeled without explicitly including electronic degrees of freedom. Atomic kinetic energies in a MD simulation are coupled via an *ad hoc* feedback loop to continuum current and heat transfer equations that are solved numerically on a finite difference grid (FDG). For resistive heating, the resistance in each region of the FDG is calculated from the experimental resistivity, atomic density, and average kinetic energy in the MD simulation. A network of resistors is established from which the potential at every FDG region is calculated given an applied voltage. The potential differences and the resistance between connected FDG regions are used to calculate the current between the two points and the heat generated from that current. This information is then added back into the atomic simulation. The method is demonstrated by simulating Joule heating and melting, along with associated changes in current, of single and bundles of metal nanowires, as well as a "pinched" wire under applied strain.

Keywords: Joule heating; Molecular simulation; Multi-scale modeling; Electron wind

1. Introduction

Joule heating plays an important role in several diverse areas of technology. These technologies include micro-electronics, where the heating of metal interconnects can play a detrimental role in device lifetime and performance [1,2]. micro-elecro-mechanical systems, where Joule heating at metal contacts can influence device performance [3] and electromagnetic launchers, where Joule heating can adversely affect the wear of the armature-rail interface [4]. Existing computational methods for modeling the influence of electric currents on atomic dynamics range from purely classical to fully quantum mechanical. In the classical models, a one-body force based on energy and momentum conservation that models collisions between moving electrons and ions (an "electron wind") is introduced into a simulation [5,6]. These models usually require specifying an effective atomic number (which can be taken as a fitting parameter), ion and electron masses and kinetic energies, and current density. They also require either simple geometries (e.g. one-dimensional current flow through wires) or some method to specify current densities. Quantum mechanical approaches for modeling Joule heating include detailed multiple scattering models [7,8], forces derived from first principles and tight binding electronic structure calculations, perturbation models, and quantum-classical Hamiltonians [6,9–16]. While more rigorous from a fundamental science viewpoint than purely classical modeling, fully quantum models are in general too computationally demanding to be used in large-scale simulations. In addition, the accuracy of these models for quantities such as heat generation and dissipation largely depends on the degree of approximation used in solving the electronic structure problem, which can add significant uncertainty into a simulation.

The solution presented here for modeling Joule heating in a large-scale molecular dynamics (MD) simulation is not to model electron dynamics, but rather to numerically solve continuum equations associated with heat transfer and current flow simultaneously with a MD simulation and couple the simulations through an *ad hoc* feedback as described below. This significantly simplifies the calculation by replacing the degrees of freedom associated with electron conduction with a coarse-grain continuum model that can be parameterized to experiment. The only input required for this approach is the experimental bulk thermal diffusivity and electrical resistivity, the applied potential, and an appropriate interatomic potential.

*Corresponding author. Clifford W. Padgett, Department of Materials Science and Engineering, North Carolina State University, Raleigh, NC 27695-7907. Tel: 919-513-2424; 919-515-7724. E-mail: cliffop@alumni.clemson.edu

Molecular Simulation
ISSN 0892-7022 print/ISSN 1029-0435 online © 2005 Taylor & Francis
http://www.tandf.co.uk/journals
DOI: 10.1080/08927020500262614

For the case discussed here, continuum heat transfer equations and electrical current relations assuming simple Ohmic behavior for an external potential are coupled to MD simulations of metals that use the embedded-atom method (EAM) interatomic forces [17]. The solution of the heat transfer equations as a continuum thermostat has been discussed earlier [18]; coupling the heating due to an electric current into the simulation is new. The validity of this method is first demonstrated by comparing the kinetic energy profile of the combined MD finite-difference (MD-FD) simulation for current flowing through a nanoscale wire with an analytic solution to this system. Two test cases are then examined. The first is a bundle of five silver nanowires in which current-induced melting and subsequent fusion into a single wire occurs. The second test case is a simulation of a "pinched" silver wire under constant strain through which a current flows with and without Joule heating. Without Joule heating in the simulation, the wire initially deforms via motion of partial dislocations. Further straining results in pinning of the dislocations, after which a short chain of single atoms forms and breaks. With sufficient Joule heating, on the other hand, the center of the wire melts, and a chain of atoms is pulled from the melt without slip in the part of the system that remains solid. While the plastic deformation of strained metal nanowires has been studied via molecular modeling, melting due to Joule heating and its influence on deformation has not been previously simulated.

2. Continuum-atomistic coupling

The method reported here builds on a continuum-atomistic thermostat previously reported [18]. In this thermostat an MD simulation is divided into grid regions (figure 1, dotted lines) and the temperature of each grid region is assigned according to the average kinetic energy of the atoms within that region. The temperature in each grid region evolves following the numerically-solved continuum heat equation

$$\frac{\partial T}{\partial t} = D\frac{\partial^2 T}{\partial R^2} + Q \tag{1}$$

where T is the temperature derived from the MD simulation, D is the thermal diffusivity, and Q is heat generated (converted to a temperature change) in the grid region from an external source (in this case current flow). The atomic velocities of the atoms in each grid region are scaled to match a numerical solution of equation (1), and the atoms are then allowed to move according to the interatomic potential with a Hoover frictional force applied locally to each grid region. This procedure is repeated, which produces a feedback between the kinetic energy of the simulation and the continuum heat transfer equation. In our initial implementation of this scheme, a straight-forward explicit finite difference method was employed so that the temperature T_{new} for each grid region is given by

$$T_{\text{new}} = T_{\text{old}} + \Delta t D\left(\sum_{\alpha}\frac{T^{\alpha}_{i+1} - 2T^{\alpha}_{i} + T^{\alpha}_{i-1}}{\Delta r_{\alpha}}\right) + Q_i \tag{2}$$

where the partial derivative in equation (1) has been approximated by a centered finite divided difference formula, Δr_{α} is the grid spacing in direction α, the sum is over the three cartesian coordinates, and i specifies the particular grid region. To conserve energy, the above equation has been modified to correct heat flows between grids containing different numbers of atoms. In this case the diffusion coefficient is multiplied by ρ_i/ρ_0, where ρ_i is the density of the neighboring grid box and ρ_0 is the density of the current grid box. This results in a variable diffusion coefficient between a grid point and its neighbors that enforces conservation of energy.

To incorporate current flow and the resulting Joule heating, a virtual network of resistors is created that connects the centers of each of the adjacent regions of the finite difference grid (FDG) (figure 1, solid lines). The resistance in each region of the FDG is calculated from the experimental resistivity and the atomic density in that region. The resistivity of each grid is defined as follows,

$$\rho_{\text{grid}} = \frac{\rho_{\text{metal}}}{d_{\text{grid}}/d_{\text{metal}} + C_{\text{air}}} \tag{3}$$

where d_{grid} and d_{metal} are the density of the current grid and bulk metal respectively, ρ_{metal} is the bulk metal resistivity, and C_{air} is a constant chosen to give ρ_{grid} the resistivity of air when d_{grid} is zero. The value of the resistor connecting two grid regions is then taken as the average resistance of the two grid regions connected

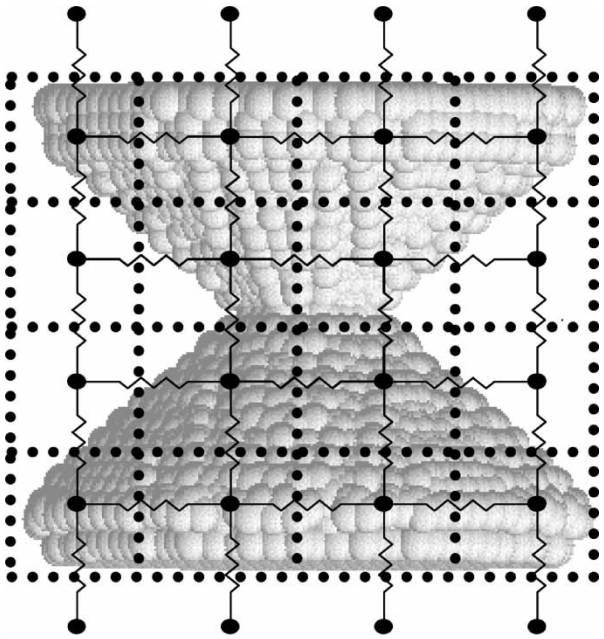

Figure 1. Describes the finite difference grid superimposed over an atomic simulation (dotted line) and the resistive network (solid lines).

by the resistor. With this virtual resistive network and an applied voltage across the system, the potential at every FDG region is calculated using a sparse matrix solver to iteratively solve Kirchhoff's law (equation (4)) using the Maxwell loop method for circuit equations [19].

$$\sum_{\alpha} i_{\alpha} = 0$$
$$\sum_{\alpha} V_{\alpha} = \sum_{\alpha} i_{\alpha} R_{\alpha} \tag{4}$$

The potential difference and the resistance between connected FDG regions is then used to calculate the current between the two points using Ohms law $V = IR$, and the heat resulting from the current flow is calculated using the power equation $P = VI$. The heat generated is then added back to the atomic velocities in the appropriate grid region via the Q term in equation (2). The MD-FD simulation is then repeated step-wise, with the grid of resistors updated as needed.

One quantity that is not specified in the equations above is the choice of appropriate grid spacing. The grid spacings must be large enough to reproduce the continuum characteristics of the current (and heat flow) equations while sufficiently small that the structural details of the system are captured. Without a specific conserved quantity, an appropriate range of grid sizes for a given simulation must be determined by trial-and-error, with grid spacings chosen such that the results are reasonably independent of the choice of grid size. This issue is further explored in the following sections.

3. Simulated Joule heating of metal nanowires

To test the numerical stability and accuracy of this coupled MD-FD scheme, simulations were carried out of current flow and resulting Joule heating due to a voltage applied across single-crystal nanowires composed of silver, aluminum, copper, gold or nickel. Two cases were examined for each metal, a temperature-independent resistivity, and a resistivity given by the equation

$$\rho_r = \rho_r(1 + \alpha_r(T - T_0)) \tag{5}$$

where ρ_{r0} is the resistivity of the metal at temperature T_0 and α is the thermal coefficient of the resistivity. For both cases the temperature at the ends of the nanowire were maintained at 300K, and temperature profiles along the wire were calculated from the MD-FD simulations as well as a numerical solution of the continuum equations without coupling to an MD simulation. In addition, for the temperature independent resistance the temperature profiles were compared to the steady-state analytic solution

$$T(x) = \frac{2g}{\lambda L} \sum_{n=1}^{\infty} \frac{\sin(x\beta_n)}{\beta_n^3} (1 - \cos(L\beta_n)) + T_0 \tag{6}$$

where λ is the thermal conductivity, L is the nanowire length, T_0 is the starting temperature of the nanowire (300K), g is the steady-state heat generation rate from the current flow, and β_n is the n^{th} root to the cosine term. Because the comparisons between the simulated temperature profiles and the profiles given by the analytic and numerical solutions to the continuum equations were similar for each metal, only the results for a silver nanowire are reported.

The MD part of the simulation was carried out with EAM potentials using a modified version of the *Paradyn* simulation code [20], which we call *ParadynEM*. The silver nanowire contained 31,563 atoms with dimensions of $200 \times 50 \times 50$ Å for the x, y, and z directions, respectively, with no periodic boundaries. The silver nanowire was first equilibrated to 300K for 10 ps using a Langevin thermostat and a time step of one femtosecond. For the initial MD-FD simulation, the simulation space was divided up into $25 \times 6 \times 6$ grid cells in the x, y, and z directions, respectively, producing a grid spacing of 8.16 Å per side in each direction. For comparison, the lattice spacing of silver is 4.09 Å in the EAM potential. Applied potentials in the range 0.01–0.10 V were used, and the ends of the wire were held at 300K. The thermal diffusivity and electrical resistivity used for the silver nanowire are 17,386 Å^2/ps and 1.4 μΩ cm, respectively, and the thermal coefficient of resistivity is taken as $\alpha = 0.0038$ μΩ cm/K.†

Plotted in figure 2 are the steady-state temperature profiles for the analytic solution (solid line), the numerical FD solution (squares) without coupling to the MD simulation, and the MD-FD simulation (triangles) for the silver nanowire with constant resistivity and a ΔV across the wire of 0.1 V. Also plotted in figure 2 are the numerical FD solution (squares) and the MD-FD simulation (triangles) results for the temperature profile with the resistivity following equation (5). For all cases, the temperature profiles calculated analytically and numerically with and without coupling to an MD simulation all agree to a very good approximation. Similar levels of agreement were seen for the range of metals and potential drops given above.

Plotted in figure 3 are temperature profiles for the same conditions as in figure 2 assuming a constant resistivity but using grid spacings of 4.08, 8.16 and 17.03 Å. For this simple geometry the temperature profiles are relatively independent of grid spacings for this range of values. For systems with more complex geometries, the results will not be accurate for grid spacings that are too large to

†Handbook where values are taken (*CRC Handbook of Chemistry and Physics*, 81st edition, CRC Press, New York, (2000).).

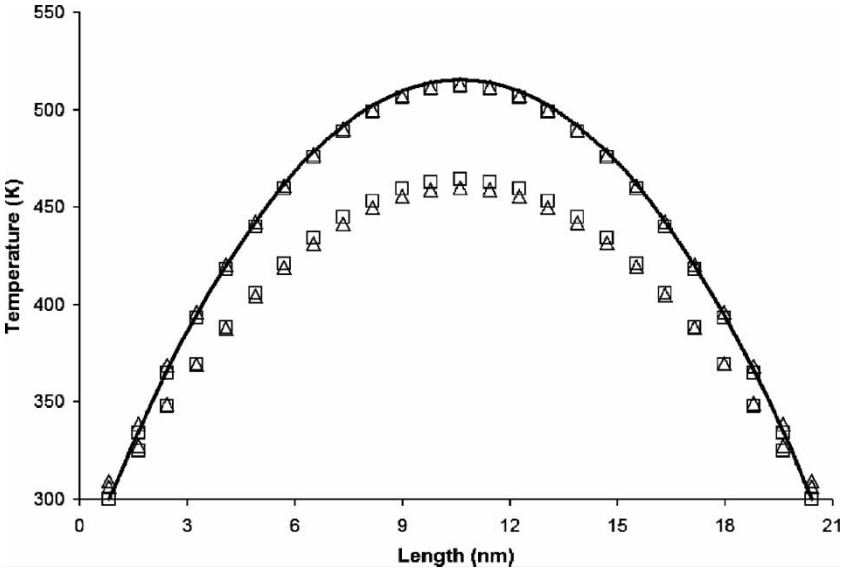

Figure 2. Kinetic energy (reported as a temperature) and temperature profiles along the silver nanowire after 1 ps of current flow with a ΔV across the wire of 0.1 V. The triangles are from the MD-FD simulations, the squares are from a finite difference solution and the solid line is the analytic solution. Top: Temperature profile generated assuming constant resistivity for silver. Bottom: Temperature profile generated assuming resistivity as a function of temperature.

appropriately capture the geometry of a given system. This is demonstrated in the next section.

4. Simulated Joule heating and melting of multiple nanowires

To model a more complex geometry, a simulation of five silver nanowires 200 Å in length and 14 Å in diameter connecting two silver plates of size 100 × 86 × 10 Å were simulated using the MD-FD approach. These wires were arranged with four at the corners and one at the center of a square approximately 30 Å per side (figure 4). This arrangement places the corner wires approximately 6 Å away from the center wire. The system, which contains 23,635 atoms, was equilibrated to 300K for 1 ps using a Langevin thermostat and a time step of one femtosecond. Applied potentials in the range 0.1–0.4 V were used, and the ends of the plates were held at 300K.

Grid sizes ranging from 4 to 20 Å per side were used in the MD-FD simulations. The simulation using the 4 Å grid size was numerically unstable. For the system using 20 Å grid sizes the temperature of the system was dominated by the constant temperature boundary conditions. The other

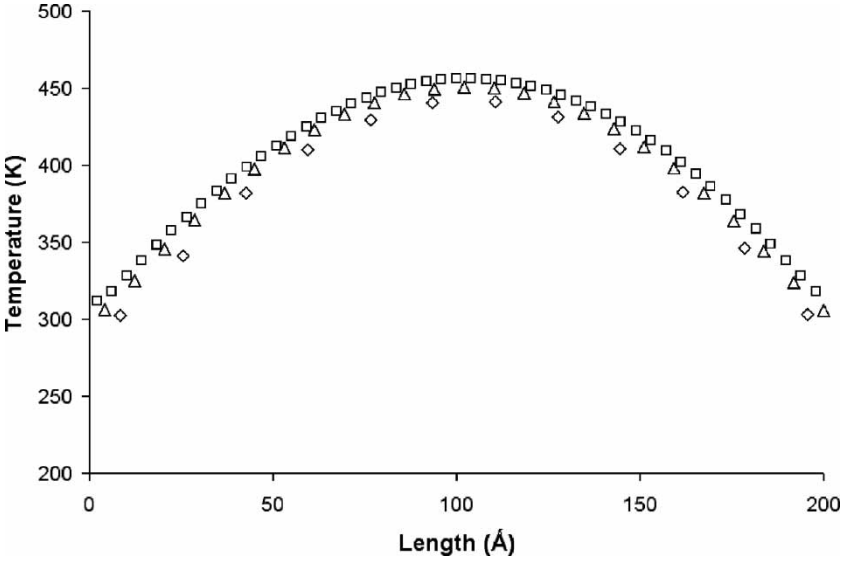

Figure 3. Temperature profile for different grid spacings. Diamonds are 17.03 Å, Triangles are 8.16 Å, and squares are 4.08 Å for a silver nanowire 200 × 50 × 50 Å, and a potential drop of 0.1 V.

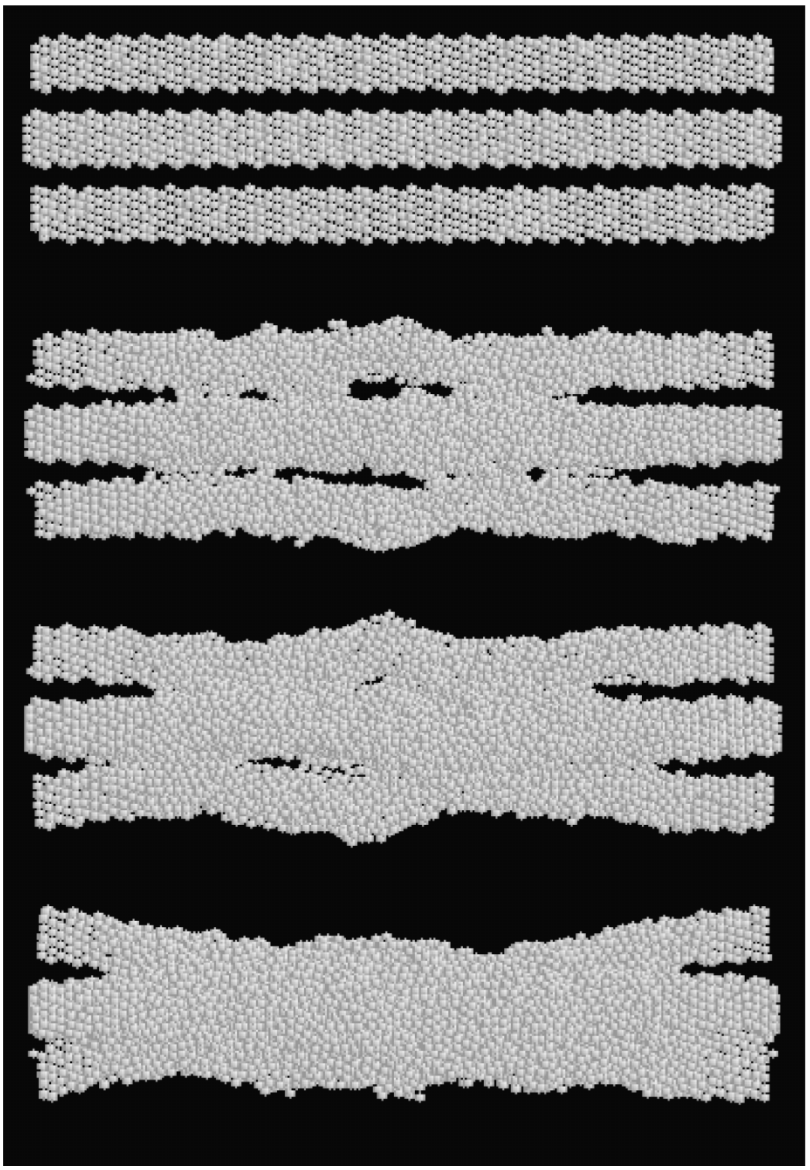

Figure 4. Snapshots from a simulation of the nanowire bundle. Snapshots were taken from top to bottom at 1, 10, 20, and 50 ps, for a simulation with a grid size of 7.1 Å and a potential drop of 0.4 V.

grid sizes examined all generated similar current and temperature plots.

The simulations ran for 50 ps, and with an applied potential of 0.4 V the temperature increased to above the melting point of silver (1235K) for the center region of the wires. Snapshots from a simulation with a grid size of 7.1 Å with an applied potential of 0.4 V are illustrated in figure 4 at four different times. Plotted in figure 5 is the average kinetic energy (reported as a temperature) for the atoms in the grids near the center of the wire as well as the total current for the system illustrated in figure 4. The current flow drops as a result of the temperature increase, and the five wires melt into one; however, no current or temperature transition was seen as the wires merged.

Plotted in figure 6 are the steady-state temperatures in the center region of the bundle and current flow through a bundle of silver nanowires as a function of potential for grid box sizes of 7.1 Å. The peak temperature increases rapidly with increased applied potential, while the current flow appears to level off. As expected, the current does not increase linearly with potential (due to the increased resistance of the heated metal), and the temperature increases nearly linearly (if current were constant power generation would be linear with applied voltage).

5. Simulated Joule heating in a strained pinched nanowire

As a final test case, a pinched silver nanowire subjected to a constant tensile strain was simulated both with and without Joule heating from current flow. As in the test cases described above, simple Ohmic behavior

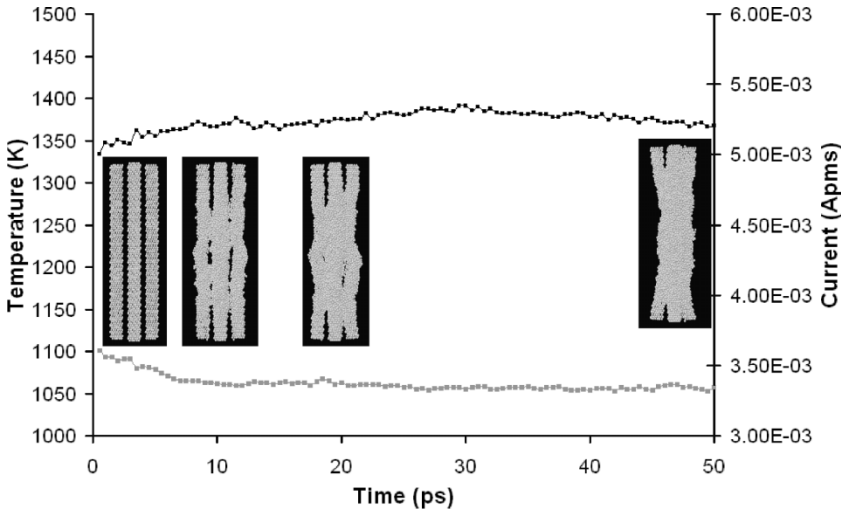

Figure 5. Describes the melting and fusion of a bundle of five silver nanowires during an atomic simulation (center wire has one in front of it and one behind it), snapshots were taken from left to right at 1, 10, 20, and 50 ps, for a simulation with a grid size of 7.1 Å and a potential drop of 0.4 V.

and continuum heat flow is assumed, and interatomic forces derived from EAM potentials are used to solve classical equations of motion for the atoms. Molecular dynamics simulations of strain-induced plastic deformation and failure of similar systems but without Joule heating have been previously reported [21–24]. For our simulations without current flow, the deformation mechanisms consist initially of motion of partial dislocations along close packed planes followed by formation of short single-atom chains before failure, consistent with prior reports. However, as shown below, the simulations reported here demonstrate that melting due to Joule heating at the region of the system with the smallest cross sectional area can significantly alter the deformation behavior of the system.

We note that prior detailed quantum mechanical calculations on metal nanowires with atomic dimensions have shown single electron transport behavior that is non-Ohmic as well as quantized phonon transport through the wire [24–27]. In principle, the Ohmic behavior assumed in the MD-FD simulation for the region of the grid surrounding the molecular chain formed due to strain can be replaced with a quantum calculation of current–voltage behavior for this region, and modifications of this type to the MD-FD method are currently being explored. For the present case, however, the assumptions of Ohmic behavior and classical heat transport are sufficient to demonstrate the MD-FD method.

The simulated system consisted initially of a pinched silver nanowire 200 Å long in the $<111>$ direction with a radius at the center of the wire of 10 Å and a radius at the two ends of 30 Å. The system contained 15,622 atoms and was equilibrated to 300K for 1 ps using a Langevin thermostat and a time step of one femtosecond.

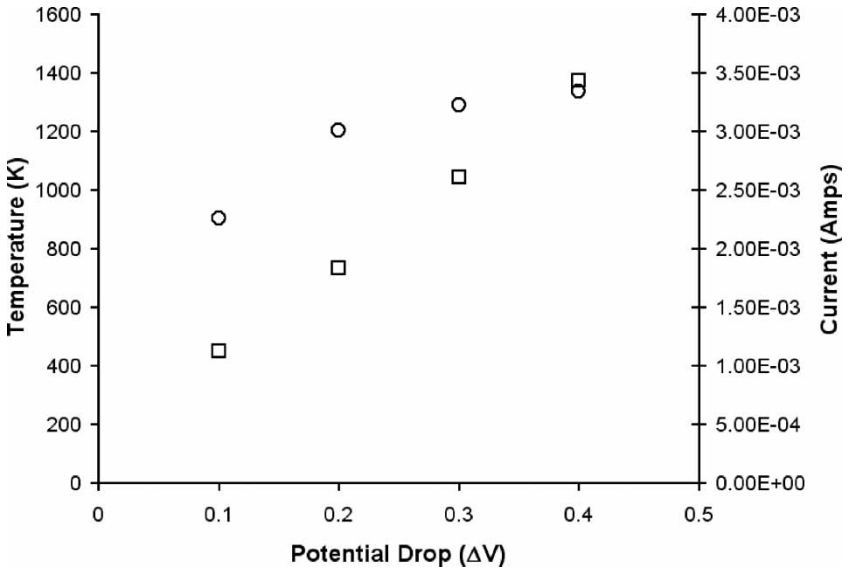

Figure 6. Steady state kinetic energy (reported as a temperature) in the center region and current flow through a bundle of silver nanowires as a function of potential for a grid box size of 7.1 Å. Current plotted as circles, temperature plotted as squares.

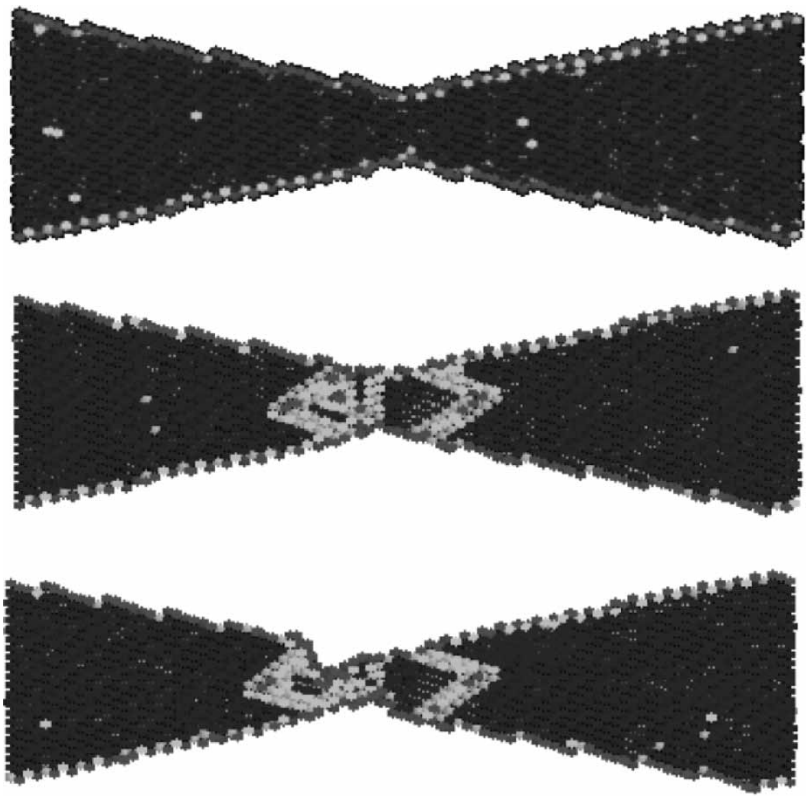

Figure 7. Snapshots of strained pinched wire without Joule heating. Atoms are colored by centrosymmetry parameter (stacking fault colored white).

For the continuum-atomistic thermostat, an applied potential of 0.4 V was used, the ends of the wire were held at 300 K, and the simulation space was divided up into grid cubes with sides of 9.1 Å. A constant strain of 0.001 Å/fs was applied to the system for 50 ps, with and without joule heating turned on.

Figure 7 describes snapshots from the system as it is strained without Joule heating. The atoms are shaded according to the symmetry of their local environment using a centro-symmetric criteria that allows stacking faults, surfaces, dislocations, and other defects to be identified in the simulation [28]. The system initially deforms by the formation of six partial dislocations, three on each side of the pinch, that start at either side of the pinch and move to the center of the wire. The dislocations, two of which are visible in the figure, travel along $<011>$-(111) slip systems until they meet and are pinned. Further deformation results in the formation of a metal "wire" a few atoms thick that breaks after approximately 35 ps.

The system that included Joule heating also formed an atomically-thin metal wire as it was strained, but via a different mechanism from the case without Joule heating. With Joule heating an approximately 40 Å long region at the center of the system melts. As the system is strained the wire forms from the melt without the initial formation of dislocations in the regions of the system that remain crystalline. This is showed in figure 8. Also in contrast to the case without Joule heating the wire did not break during the course of the simulation, but rather it continued to be drawn from the melted region.

Plotted in figure 9 are temperatures in the center region of the wire and current flow through the wire as a function of time for the two systems illustrated in figures 7 and 8 (temperature for the case without Joule heating was constant at 300K and is therefore not plotted). As expected, current flow abruptly stops in the case without Joule heating incorporated into the simulation when the wire breaks. For the system with Joule heating, the current is reduced as the wire is drawn further, but does not go to zero, again as expected.

6. Conclusions

A new method for incorporating Joule heating into a classical MD simulation has been presented in which continuum equations for thermal transport and heat generation from current flow are numerically solved simultaneously with a MD simulation, with an *ad hoc* feedback between the two simulations. This method allows heating due to current flow to be included in MD simulations without explicitly treating electronic degrees of freedom, a critical feature for large-scale systems.

Three test cases were used to characterize this method. The first test case was Joule heating of a single nanowire with and without a temperature dependent electrical resistivity. The calculated temperature profiles

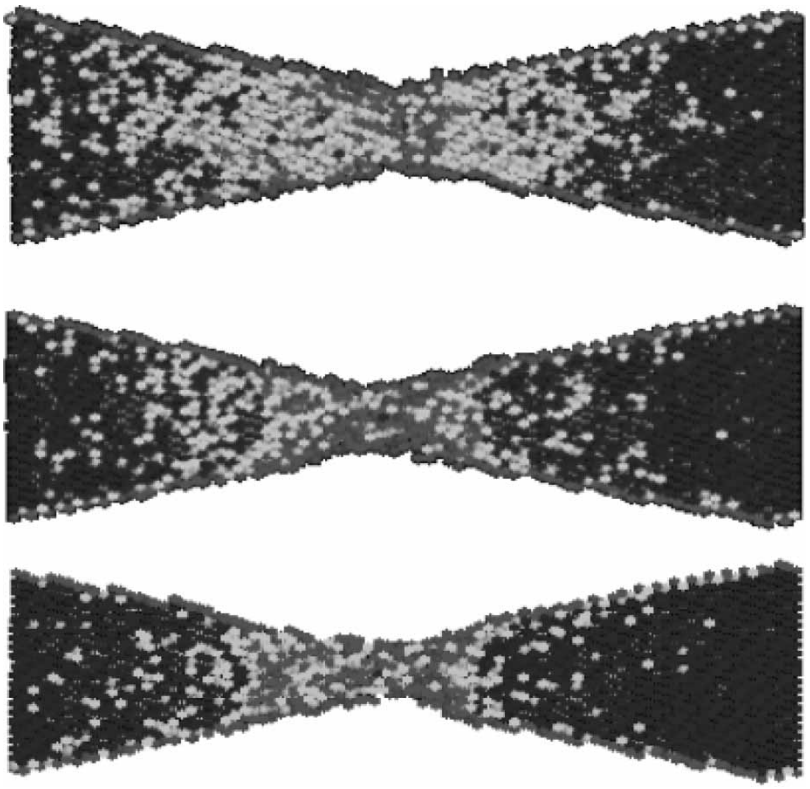

Figure 8. Snapshots of the strained pinched wire with Joule heating with atoms colored by centrosymmetry parameter.

with a constant resistivity were found to compare well with analytic solutions for this case. For temperature dependent resistivities, the FD and coupled MD-FD solutions agree with one another, supporting the numerical stability of the coupling scheme. The second two test cases were the melting and coalescence of five silver nanowires into a single wire due to Joule melting, and the tensile strain of a pinched silver nanowire with and without Joule heating. For the pinched junction, formation of a single-atom chain due to the applied strain was observed in the simulations both with and without Joule heating. The mechanisms, however, were different for the two cases,

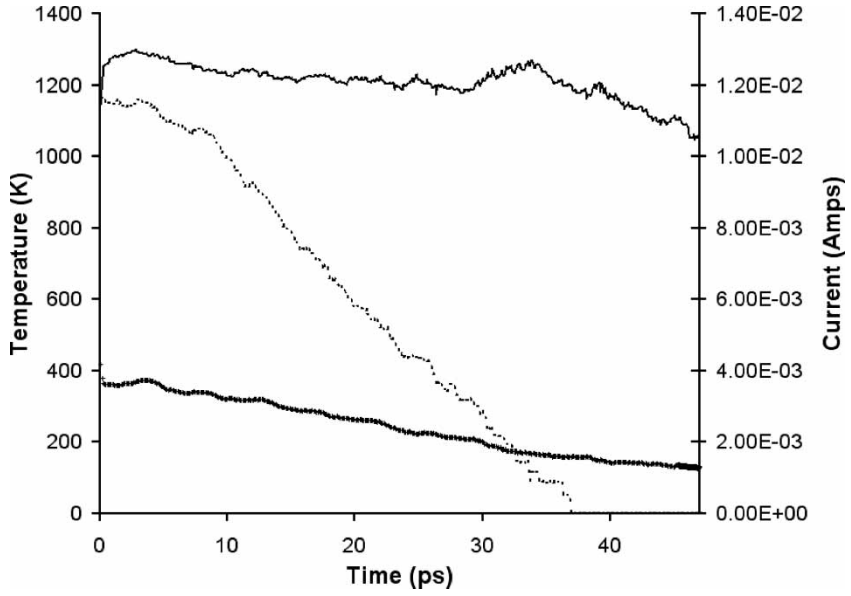

Figure 9. Kinetic energy (reported as a temperature) in the center region and current flow through a pinched silver nanowire under constant strain as a function of time for a grid box size of 9.1 Å, and an applied potential of 0.4 V. Current plotted as dashes for the case with no Joule heating, and with pluses with Joule heating. The temperature, which is plotted as a solid line, is for case with Joule heating.

with initial formation of partial dislocations observed without Joule heating, and wire formation from a melted region at the pinch with Joule heating.

We note that with this approach, current densities throughout a simulation can be estimated from the solution to the network of resistors. These current densities can in turn be used to estimate classical electron wind forces such as those mentioned in the introduction. In addition, electromagnetic fields outside of the region occupied by atoms can be numerically calculated from the current densities. These fields can be used to incorporate into large-scale MD simulations effects such as ionization probabilities for surface atoms [28], ion trajectories, and magnetic "blow-off" forces due to current flow through tapered wires [29], opening a host of atomic-level phenomena to simulation. Also, as mentioned above, it is in principle possible to replace the Ohmic behavior assumed here with nonlinear current–voltage relations calculated from quantum transport calculations in localized grid regions. These and similar capabilities are currently being explored.

Acknowledgements

This work was funded by a Georgia Tech MURI, which is supported by the Office of Naval Research. Helpful discussions with J. David Schall, George C. Jordan, Doug Irving, and Yanhong Hu are acknowledged.

References

[1] See for example K.E. Goodson. Thermal conduction in electronic microstructures. In *Thermal Engineering Handbook*, F. Kreith (Ed.), CRC Press, Boca Raton, Florida (2000).
[2] E. Misra, C. Marenco, N.D. Theodore, T.L. Alford. Failure mechanisms of silver and aluminum on titanium nitride under high current stress. *Thin Solid Films*, **474**, 235 (2005).
[3] S.T. Patton, J.S. Zabinski. Fundamental studies of Au contacts in MEMS RF switches. *Tribol. lett.*, **18**, 215 (2005).
[4] See for example G.A. Shvetsov, V.M. Titov. Railgun accelerators of macroparticles: Hopes and reality. In *Megagauss Fields and Pulsed Power Systems*, V.M. Titov, G.A. Shvetsov (Eds.), pp. 767–772, Nova Science, New York (1987).
[5] S. Shingubara, I. Utsunomiya, T. Takahagi. Interaction of a void and a grain boundary under a high electric current stress employing three-dimensional molecular dynamics simulation. *Appl. Surface Sci.*, **91**, 220 (1995).
[6] A.P. Horsfield, D.R. Bowler, A.J. Fisher, T.N. Todorov, M.J. Montgomery. Power dissipation in nanoscale conductors: Classical, semi-classical and quantum dynamics. *J. Phys. Condens. Mat.*, **16**, 3609 (2004).
[7] P.J. Rous. Driving force for adatom electromigration within mixed CuAl overlayers on Al(111). *J. Appl. Phys.*, **89**, 4809 (2001).
[8] P.J. Rous. Electromigration wind force at stepped Al surfaces. *Phys. Rev. B*, **59**, 7719 (1999).
[9] T.N. Todorov. Local heating in ballistic atomic-scale contacts. *Phil. Mag. B*, **77**, 965 (1998).
[10] J. Hoekstra, A.P. Sutton, T.N. Todorov, A.P. Horsfield. Electromigration of vacancies in copper. *Phys. Rev. B*, **62**, 8568 (2000).
[11] T.N. Todorov. Time dependent tight binding theory. *J. Phys. Condens. Mat.*, **13**, 10125 (2001).
[12] T.N. Todorov. Tight-binding simulation of current-carrying nanostructures. *J. Phys. Condens. Mat.*, **14**, 3049 (2002).
[13] M.J. Montgomery, T.N. Todorov, A. P. Sutton. Power dissipation in nanoscale conductors. *J. Phys. Condens. Mat.*, **14**, 5377 (2002).
[14] M. Brandbyge, K. Stokbro, J. Taylor, J.-L. Mozos, P. Ordejo. Origin of current-induced forces in an atomic gold wire: A first-principles study. *Phys. Rev. B*, **67**, 193104 (2003).
[15] Y.C. Chen, M. Zwolak, M. Di Ventra. Local heating in nanoscale conductors. *Nano Lett.*, **3**, 1691 (2003).
[16] A.P. Horsfield, D.R. Bowler, A.J. Fisher. Open-boundary Ehrenfest molecular dynamics: towards a model of current induced heating in nanowires. *J. Phys. Condens Mat*, **16**, L65 (2004).
[17] M.S. Daw, S.M. Foiles, M.I. Baskes. The embedded atom method—a review of theory and applications. *Mat. Sci. Rep.*, **9**, 251 (1993).
[18] J.D. Schall, C.W. Padgett, W. Brenner. *Ad hoc* continuum-atomistic thermostat for modeling heat flow in molecular dynamics simulations. *Mol. Simul.*, **31**, 283 (2005).
[19] See for example A.F. Kip. Appendix G, The Maxwell loop method for circuit equations. In *Fundamentals of Electricity and Magnetism*, McGraw-Hill, New York (1969).
[20] S.J. Plimpton, B. A. Hendrickson. Parallel molecular dynamics with the embedded atom method. *Mat. Res. Soc. Symp. Proc.*, **291**, 37 (1993).
[21] U. Landman, W.D. Luedtke, N.A. Burnham, J. Colton. Atomistic mechanisms and dynamics of adhesion nanoindentation and fracture. *Science*, **248**, 454 (1990).
[22] E.Z. da Silva, A.J.R. da Silva, A. Fazzio. How do gold nanowires break? *Phys. Rev. Lett.*, **87**, 256102 (2001).
[23] J.K. Diao, K. Gall, L. Dunn. Yield strength in asymmetry in metal nanowires. *Nano Lett.*, **4**, 1863 (2004).
[24] H. Hakkinen, R.N. Barnett, A.G. Scherbakov, U. Landman. Nanowire gold chains: Formation mechanisms and conductance. *J. Phys. Chem. B*, **104**, 9063 (2000).
[25] S. Ciraci, A. Buldum, I. P. Batra. Quantum effects in electrical and thermal transport through nanowires. *J. Phys. Condens. Matter*, **13**, R537 (2001).
[26] D.M. Gillingham, I. Linington, C. Muller, J.A.C. Bland. e^2/h quantization of the conduction in Cu nanowires. *J. Appl. Phys.*, **93**, 7388 (2003).
[27] M. Zhuang, M. Ernzerhof. Zero-voltage conductance of short gold nanowires. *J. Chem. Phys.*, **120**, 4921 (2004).
[28] See for example H.J. Kreuzer. Physics and Chemistry in high electric fields. *Surface and Interface Anal.*, **36**, 372 (2004).
[29] See for example F.C. Moon. Chapters dealing with Nanoelectrical contact stability. In *Magneto-Solid Mechanics*, Wiley, New York (1989).